1996

Atomic force microscopy reconstruction of G-wire DNA

James Vesenka
Iowa State University

Thomas Marsh
University of Wisconsin - Green Bay

Richard Miller
Iowa State University

Eric Henderson
Iowa State University, telomere@iastate.edu

Atomic force microscopy reconstruction of G-wire DNA[a)]

James VesenkaThomas MarshRichard MillerEric Henderson

Citation: Journal of Vacuum Science & Technology B: Microelectronics and Nanometer Structures Processing, Measurement, and Phenomena **14**, 1413 (1996); doi: 10.1116/1.589110

View online: http://dx.doi.org/10.1116/1.589110

View Table of Contents: http://avs.scitation.org/toc/jvn/14/2

Published by the American Institute of Physics

Atomic force microscopy reconstruction of G-wire DNA[a)]

James Vesenka[b)]
Department of Zoology and Genetics, Iowa State University, Ames, Iowa 50011 and BioForce Laboratory, Ames, Iowa 50014

Thomas Marsh
Department of Life Science, University of Wisconsin, Green Bay, Wisconsin 54311

Richard Miller
Department of Mathematics, Iowa State University, Ames, Iowa 50011

Eric Henderson
Department of Zoology and Genetics, Iowa State University, Ames, Iowa 50011 and BioForce Laboratory, Ames, Iowa 50014

(Received 24 July 1995; accepted 9 November 1995)

A fundamental problem in atomic force microscopy (AFM) image interpretation is distinguishing features arising from tip geometry from true molecular detail. In this study, a novel 4-stranded form of DNA (the ''G wire'') was coadsorbed with 7.6-nm-diam colloidal gold probe calibration standards and examined by AFM. After the probe apices were reconstructed from AFM images of the standards, the artificial broadening of the coadsorbed G-wire DNA was removed, resulting in more reliable image interpretation. Using simple geometric models, a favorable comparison between observed and modeled G-wire cross sections suggests that reconstructions removed about 25% of the tip-broadened AFM image in these studies.

I. INTRODUCTION

Evidence of artificial broadening of biomolecular shape due to finite apical tip geometry has been observed since the first atomic force microscope (AFM) images of plasmid DNA were made.[1–8] Numerous algorithms have been developed to compensate for tip broadening.[9–15] In this article we apply the procedure of Miller and co-workers[11] to the reconstruction of images of a novel form of quadruplex DNA (G wires[16]) by first accurately determining the tip shape from coadsorbed colloidal gold particles,[13,17] followed by reconstruction of the entire image. The voracity of the algorithm is tested by comparing the volume per unit length of G wire (i.e., G-wire cross section) from experimental results with the cross section image reconstruction of a hemispherical tip in contact with a *rigid* cylindrical rod of G-wire DNA lying on its side on mica.

The emphasis on rigid here is intentional. Several articles on AFM of DNA[1–3,7,8] indicate the imaged DNA to be less than half the 2.0 nm height of its x-ray determined diameter. The smaller diameter has been suggested to be the result of cationic bridges to the mica substrate[16] or due to stretching the DNA,[18] both a result of inherent duplex DNA flexibility. Marsh and co-workers[16] have shown that the quadruplex DNA is much more rigid, closely retaining (within 25%) the 2.4-nm-diam observed by x-ray techniques when imaged by AFM.

II. MATERIALS AND METHODS

$G_4T_2G_4$ oligonucleotide (Midland Certified), or ''oligo,'' was purified on a 12% polyacrylamide gel. The oligo was cut from the gel, diced, eluted into 10 mM Tris-EDTA (*p*H 7.5), and the gel fragments centrifuged out. The supernatent was then purified on a C18 column to remove excess salt. The oligo was eluted in 50/50 methanol/water and dried down. The dried sample was resuspended in water, incubated at 95 °C to fully denature the molecule, and diluted (0.25 μg/ml) into self-assembly buffer (10 mM Tris *p*H 7.5, 5 mM $MgCl_2$, and 50 mM NaCl or KCl) and incubated for 24 h at 37 °C. G wires that form in this time can be diluted 1:100 into an AFM buffer (10 mM Tris, 1 mM $MgCl_2$, *p*H 7.5) with 1:10 stock dilution of gold particles (Ted Pella, Inc.) and directly deposited onto freshly cleaved mica. After incubating 5 min, excess sample was rinsed off the mica with 1 ml distilled water, vigorously blown dry with nitrogen, and imaged with a Nanoscope III AFM (Digital Instruments). Images were taken in Tapping Mode™ in dry air (relative humidity $<$10%) with single crystal silicon 125-μm-long tapping tips (Nanoprobes). The images were flattened to make the background have the same height (gray scale) and were then reconstructed with an algorithm developed by Miller and co-workers.[11]

Volume measurements were made using macros developed for NIH Image, version 1.57. The volume measurements are taken by defining the substrate's background out of 256 gray levels and summing up the area under each pixel of the sample above the background, calibrated to the known vertical height scale. Consequently, the largest source of error comes from defining the substrate plane (a minimum of 10% in these volume measurements). The lateral and vertical height calibrations have less than 5% error and are ignored in

[a)]Journal Paper No. J-16456 of the Iowa Agriculture and Home Economics Experiment Station, Ames, Iowa; Project No. 3064.
[b)]To whom all correspondence should be addressed. Present address: Physics Department, California State University, Fresno, CA 93740-0037.

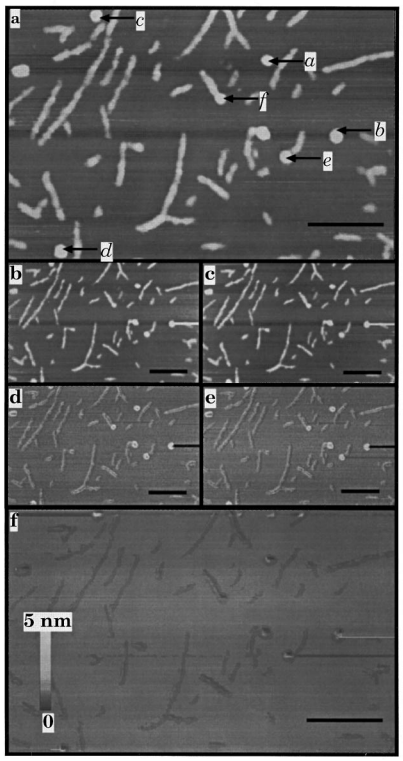

FIG. 1. (a) Typical raw image of G-wire DNA coadsorbed with 7.6±0.9 nm colloidal gold particles. Letters near particles reference topographic reconstructions in Fig. 2. (b) and (c) Typical reconstructed images of (a) employing particles (b) and (e). The streak adjacent to one of the particles is an artifact of the reconstruction process. (d) and (e) are difference images [(a)−(b), (a)−(c)] showing the amount of reconstructed volume claimed by the reconstruction process. (f) The ''second'' difference image of (b)−(c) or (d)−(e). The vertical gray scale (0–5 nm) in all six images is set to enhance the height of the DNA, making the gold particles appear to be bleached out. The black scale bar is 100 nm for all six panels.

making the error estimate. The volumes of the gold particles are subtracted from the total volume. The resulting number is then divided by the total linear length of G wire in the image field to obtain the raw and reconstructed volume/unit length (cross section) of G-wire DNA.

III. RESULTS AND DISCUSSION

A typical image of G-wire DNA coadsorbed with 7.6±0.9 nm colloidal gold particles is shown in Fig. 1(a). Figures 1(b) and 1(c) are typical reconstructed images of Fig. 1(a) employing particles b and e. The streaks adjacent to two of the larger particles are artifacts due to the reconstruction process. The reconstruction procedure is a two step process:

(1) Reconstruct the tip from a characteristic gold particle (the chosen gold particle should have symmetry similar to other gold particles in the field to ensure reasonable reconstructions). The gold particles must be at least three times the average height of the sample, since only about a third of the gold particle's height is in contact with the tip.[13] In our system, the G wire averaged 2.0±0.5 nm and the gold particles were 7.6±0.9 nm.

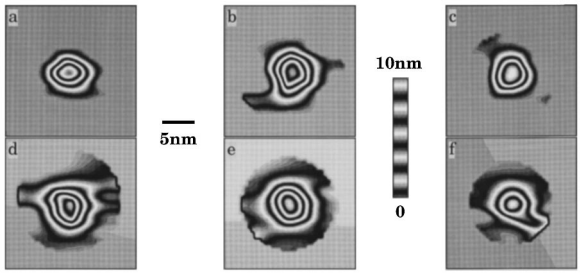

FIG. 2. Panel of six different reconstructions of the same tip from four different gold particles [numbered in Fig. 1(a)]. The contour map shows approximately 2 nm of vertical height change between each pair of black and white bars.

(2) Reconstruct the image based on the known tip shape. The reconstruction starts from the tallest feature on the field and moves in a single pass parallel to the slow scan axis followed by reconstruction of each fast scan line. The assumption is that the gold particle from which the tip is reconstructed is the tallest structure. Consequently, other tall structures, if not nearby, can give rise to reconstruction artifacts (streaks).

Figure 1 compares a raw and reconstructed field of G-wire DNA and gold. Note the marginal slimming of the G-wire DNA that can be seen in the top view images of Figs. 1(b) and 1(c). The vertical gray scale (0–5 nm) in all six images is set to enhance the height of the DNA, making the gold particles appear bleached out. Figures 1(d) and 1(e) are difference images [Figs. 1(a)−1(b), Figs. 1(a)−1(c)] that identify the volume claimed by the reconstruction process. Notice also the donut-shaped structures surrounding the gold particles and raised furrows surrounding the G wires. These structures indicate that the tallest features from each reconstructed gold particle and G-wire map 1:1 with the raw data, and the sides of the unreconstructed gold particles and G wire are due to tip artifact. Whereas the G wires are reconstructed from tip information, the edges of the gold particles are reconstructed from an extrapolated tip shape, making the image reconstruction of the gold particles unreliable around the edges of each particle.

Figure 1(f) is the ''second'' difference image between Figs. 1(c) and 1(e). The purpose of this image is to show that reconstructions from different particles give similar results, and therefore a nearly zero second difference is observed. This is to be expected from the uniform gold particles that are used to reconstruct the tip (see Fig. 2). The volume of this second difference is smaller than the error surrounding the measuring process (see Table I).

Figure 2 is a panel of six different reconstructions of the same tip from four different gold particles [lettered in Fig. 1(a)]. The contour map shows approximately 2 nm of vertical height change between each pair of black and white bars. The vertical and lateral height scale is the same for all six images. The edges of each tip reconstruction vary between particles and reflect local variations between the particle and substrate topography. The apex of each reconstruction of the same tip also differs, suggesting either a continuously chang-

TABLE I. The top three rows contain representative contact heights, theoretical raw, and reconstructed G-wire DNA volume/unit lengths (cross sections), difference between the two areas, and estimated unreconstructed volume of an average gold particle. The bottom rows are experimental results and error with details explained by the alphabetical superscripts. Calculations based on 2.0±0.5 nm G wires and 7.6±0.9 nm average height of gold.

R_c(nm)	h(nm)	A_u(nm^2)	A_r(nm^2)	ΔA(nm^2)	V_u(nm^3)
20.000	1.9048	19.070	13.847	5.223	3169
10.000	1.8182	13.255	10.876	2.379	1354
5.0000	1.6667	9.0267	8.7875	0.0239	448
8.5±1.1	NA	12.4±1.6	9.4±1.3	3.0±0.6[a]	1100±140
				2.5±1.0[b]	
				0.2±0.4[c]	

[a]Calculated by subtracting reconstructed from raw data cross sections.
[b]Directly measured from difference images [Fig. 2(d) or 2(e)].
[c]Directly measured from second difference images [Figs. 2(b)−2(c)=2(d)−2(e)=2(f)].

ing tip geometry or nonuniformity of the gold particles. It is difficult to determine the predominating factor. Though it is well known that the geometric characteristics of colloidal gold particles are batch dependent, our batch was rigorously characterized by transmission electron microscopy (TEM) and had a standard deviation of less than 10% both in size and ellipticity. Future efforts will be focused on employing other types of uniformly round standards. Colloidal gold has been used here because it is inexpensive, easy to coadsorb with a sample, and tends not to bind to the sample. Greater improvements in maintaining a standard spherical character without compromising adhesion and sample contamination are needed. These improvement could help to map out subtle changes in tip geometry as the tip scans the surface and picks up and drops off sample residue during the imaging process.

Figure 3 compares reconstructed tip cross sections from two gold particles [Figs. 2(b) and 2(e)]. The notable feature is that although the two reconstructions appear to have very different surface topographies on the nanometer scale, their multinanometer scale features (radius of curvatures as a function of cross section viewpoint) are in excellent agreement. Each reconstruction is viewed from two orthogonal directions (indicated by the arrows). The radius of curvature from Figs. 3(b) and 3(e) both are about 8.5±1.0 nm, whereas Figs. 3(c) and 3(f) are 5.0±1.0 nm. Even at the extremes of the error limits, the two radii of curvature are distinct, and consistent with other tip reconstructions from Fig. 2 (data not shown), providing strong evidence for subtle asymmetry of the tip shape that is not immediately apparent from direct observation of the colloidal gold particles in the raw AFM image. In an effort to further determine the efficacy of the image reconstruction algorithm a simple geometric model, based on easily measured features of the G wires and tip, was employed to compare the reduction in the volume/unit length (cross section) of G wire due to the reconstruction process. The model was then compared with experimental data and found to be in good agreement.

IV. IMAGE RECONSTRUCTION MODEL

Figure 4(a) is a model of the key components for comparison with the area under reconstructed volume/unit length (cross section). $\theta/2$ is the half-angle between the substrate normal and the line intersecting the tip's hemispherical origin and the center of the G-wire DNA (modeled as a cylindrical rod lying flat on its side). R_c is the radius of curvature of the tip, H is the height of the DNA above the mica substrate, and h is the height of the contact point between the tip

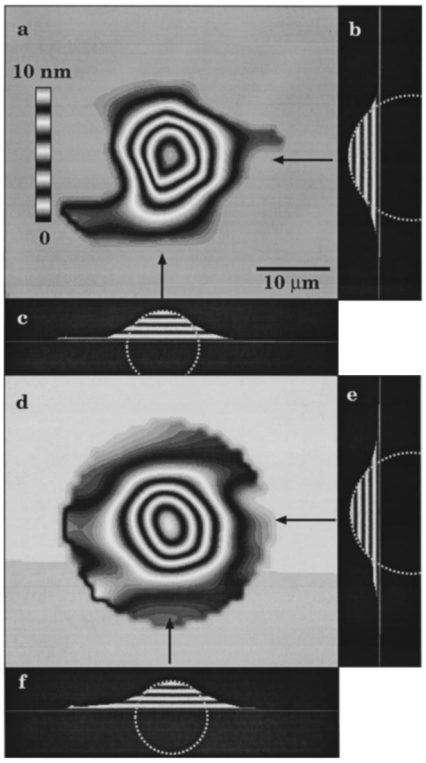

FIG. 3. Top view and side view images from particles (b) and (e) [see Fig. 1(a)]. The superimposed circle is 8.5 nm in radius of curvature in (b) and (e) and 5.0 nm radius of curvature in (c) and (f). The scale bar in (a) is 10 nm.

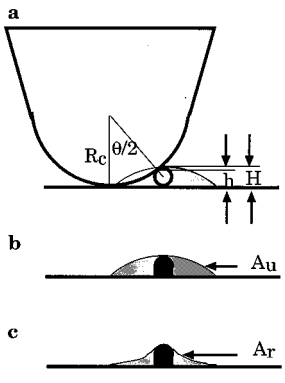

FIG. 4. (a) Model of the key components for the cross sectional image reconstruction components. (b) The approximate unreconstructed cross section A_u due to the tip's apex mapping out an image of the smaller G-wire DNA (black silhouette). (c) The reconstructed cross section A_r when the shape of the tip is removed from (b). The black silhouette in the middle of (b) and (c) is the cross sectional shadow of the G-wire DNA expected for an ideal (delta function) tip.

on the DNA. Figure 4(b) is the unreconstructed cross section A_u due to the tip's apex mapping out the AFM image above the smaller G-wire DNA (black silhouette). Figure 4(c) is the reconstructed cross section A_r of the AFM image when the shape of the tip is removed from Fig. 3(b). The black silhouette in the middle of Figs. 4(b) and 4(c) is the cross sectional shadow of the G-wire DNA expected for an ideal (delta function) tip normally incident upon the substrate. Notice that even after reconstruction, the majority of cross sectional area is largely represented by a region of lost information, where the apex of the tip is not in contact with sample.

In order to estimate the area under unreconstructed (raw) and reconstructed cross sections, the contact height and contact angle must be calculated in terms of H and R_c:

$$h=\frac{2R_cH}{2R_c+H}, \tag{1}$$

$$\theta=2\cos^{-1}\left(\frac{R_c-h}{R_c}\right). \tag{2}$$

The unreconstructed cross sectional area from analytical geometry is [Fig. 4(b)]

$$A_u(\mathrm{nm}^2)=\frac{R_c^2\theta}{2}-(R-H)\sqrt{2R_cH-H^2}, \tag{3}$$

where θ is in radians. The reconstructed area [Fig. 4(c)] is given by

$$A_r(\mathrm{nm}^2)\approx(R+h)\sqrt{2R_ch-h^2}-\frac{R_c^2\theta}{2}+2hH\sin\left(\frac{\theta}{2}\right). \tag{4}$$

The unreconstructed volume surrounding a gold particle is the three dimensional analog of Eq. (3) and is given by

$$V_u=\frac{\pi}{3}H^2(3R_c-H). \tag{5}$$

The mailbox-shaped cross section under the G-wire DNA is estimated by a 2-nm-diam semicircular cap, $0.5\pi r^2$, with a rectangular base $2r^2=0.5\pi(1\ \mathrm{nm})^2+2\ \mathrm{nm}^2\approx3.6\ \mathrm{nm}^2$.

Table I summarizes the theoretical and experimental measurements of G-wire cross sections and colloidal gold unreconstructed volumes. No comparison of reconstructed particle volumes is made with theory because the reconstructed gold particles are made from extrapolated, rather than genuine, tip features. The basic observations are as follows:

(1) An estimate of the tip radius of curvature from the averaged unreconstructed reduction of colloidal gold volumes through Eq. (5) is 8.5 ± 1.1 nm and is in good agreement with the tip reconstructions of Figs. 3(b) and 3(e).

(2) For comparison purposes, three different estimates of raw and reconstructed cross sections are included based on tips with radius of curvature of 20, 10, and 5 nm (top three lines of Table I). The summarized experimental data are included in the last row and are within experimental error of the modeled cross sections.

The experimental data for raw and reconstructed cross sections fall between the theoretical estimates for 2-nm-diam (tall) G-wire DNA and tips with radius of curvature of 5 and 10 nm. The difference between raw and reconstructed cross sections (3.0 ± 1.0 nm) falls between the 10 and 20 nm radius of curvature limit, though we would expect it to be lower based on the sharper tip geometries seen in Figs. 3(c) and 3(f). The smaller 2.5 ± 1.0 nm difference is an actual measure of the difference volume from Figs. 1(d) or 1(e). The large error overlaps the directly calculated difference. The cross section area difference of 0.2 ± 0.4 nm reflects a height comparison between Figs. 1(b) and 1(c) or 1(d) and 1(e). The error being larger than the volume measurement suggests that reconstructions from different particles give similar results.

Image reconstruction provides a small improvement (25%) of the reduction in volume due to tip geometry for G-wire DNA. The area of the region of indeterminacy [Fig. 3(c)] is larger (5.8 nm^2 for our system) than the area under the actual sample (about 3.6 nm^2) and would continue to deteriorate with increasing sample height. Identification of this region of indeterminacy remains an area of current research in our laboratory. An indication of how little of the sample is imaged by the tip can be seen in Table I under column labeled h, the height of the sample where the tip makes contact. Even for a very sharp tip (5 nm), only the top sixth of a 2 nm tall sample is imaged. The solution to high resolution AFM imaging of larger biomolecules still awaits improvements in tip manufacturing and sharpening processes. The reconstruction algorithm used here may have some advantage in an area of experimentation where subtle changes in tip shape, perhaps due to adsorption/desorption processes, need to be detected. Further improvements in calibration standards will be needed for more reliable tip and image reconstruction.

V. CONCLUSIONS

Image reconstructions of G-wire DNA were made using colloidal gold standards to reconstruct the tip shape. The uniformity of the reconstructions could be seen through comparisons of the tip geometry and differences between volume/unit lengths of G wire reconstructed from different gold particles. A 25% reduction in volume in the reconstructed images were obtained. For the tips used in this study, the region of indeterminacy, i.e., the region of sample not contacted by the tip's apex, was larger than the volume of the modeled sample.

ACKNOWLEDGMENTS

This research was supported in part by NSF Signal Transduction Training Grant No. DIR-9113595. The authors thank Rick Giberson of Ted Pella, Inc. for providing the colloidal gold standards used in these experiments. The volume measurement NIH Image was developed by Wolfgang Fritzsche. The authors thank Marc Porter (Iowa State University) for the use of the Tapping Mode™ AFM.

[1]M. J. Allen, N. V. Hud, M. Balooch, R. J. Tench, W. J. Siekhaus, and R. Balhorn, Ultramicrosc. **42–44**, 1095 (1992).
[2]C. Bustamante, J. Vesenka, C. L. Tang, W. Rees, M. Guthold, and R. Keller, Biochem. **31**, 22 (1992).

[3]H. Hansma, J. Vesenka, C. Siegerist, G. Kelderman, H. Morret, R. L. Sinsheimer, V. Elings, C. Bustamante, and P. K. Hansma, Science **256**, 1180 (1992).
[4]E. Henderson, Nucleic Acids Res. **20**, 445 (1992).
[5]Y. L. Lyubchenko, A. A. Gall, L. S. Shlyakhtenko, R. E. Harrington, B. L. Jacobs, P. I. Oden, and S. M. Lindsay, J. Biomol. Struct. Dynam. **10**, 589 (1992).
[6]T. Thundat, D. P. Allison, R. J. Warmack, and T. L. Ferrell, Ultramicrosc. **42–44**, 1101 (1993).
[7]J. Vesenka, M. Guthold, C. L. Tang, D. Keller, C. Delaine, and C. Bustamante, Ultramicrosc. **42–44**, 1243 (1993).
[8]F. Zenhausern, M. Adrian, B. ten Heggerler-Bordier, R. Emch, M. Jobin, M. Taborelli, and P. Descouts, J. Struct. Biol. **108**, 69 (1992).
[9]D. J. Keller and F. S. Franke, Surf. Sci. **294**, 409 (1993).
[10]P. Markiewicz and M. C. Goh, Langmuir **10**, 5 (1994).
[11]R. Miller, E. Henderson, and J. Vesenka, SIAM J. Math (to be published).
[12]G. S. Pingali and R. Jain, Proceedings of the IEEE Workshop on Applications of Computer Vision (unpublished).
[13]J. Vesenka, R. Miller, and E. Henderson, Rev. Sci. Instrum. **65**, 2249 (1994).
[14]J. Villarrubia, Surf. Sci. **321**, 287 (1994).
[15]P. M. Williams, K. M. Shakesheff, M. C. Davies, D. E. Jackson, C. J. Roberts, and S. J. B. Tendler (unpublished).
[16]T. Marsh, J. Vesenka, and E. Henderson, Nucleic Acids Res. **23**, 696 (1995).
[17]J. Vesenka, S. Manne, R. Giberson, T. Marsh, and E. Henderson, Biophys. J. **65**, 992 (1993).
[18]T. Thundat, D. P. Allison, and R. J. Warmack, Nucleic Acids Res. **22**, 4224 (1994).